# Melting and crystallization features of CsPbBr 3 perovskite

Andrii Kanak, Oleg Kopach, Liliia Kanak, Ievgen Levchuk, Mykola Isaiev, Christoph Brabec, Petro Fochuk, Yuriy Khalavka

# Melting and crystallization features of $CsPbBr_3$ perovskite

*Andrii Kanak[1]*, Oleg Kopach[1], Liliia Kanak[1], Ievgen Levchuk[2],Mykola Isaiev[3], Christoph J. Brabec[2,4], Petro Fochuk[1], Yuriy Khalavka[1]*

[1]Yuriy Fedkovych Chernivtsi National University, Department of General Chemistry and Chemistry of Materials, 2 Str. Kotsyubynsky, 58002, Chernivtsi, Ukraine

[2]Institute of Materials for Electronics and Energy Technology (i-MEET), Department of Materials Science and Engineering, Friedrich-Alexander University Erlangen-Nürnberg, Martensstrasse 7, 91058, Erlangen, Germany

[3]Université de Lorraine, CNRS, LEMTA, F-54000 Nancy, France

[4]Helmholtz-Institute Erlangen-Nürnberg for Renewable Energy (HI ERN), Immerwahrstr. 2, 91058, Erlangen, Germany

KEYWORDS: $CsPbBr_3$, melting, crystallization, Phase transition, heating/cooling rate

**ABSTRACT**

All-inorganic perovskite $CsPbBr_3$ has attracted considerable attention as a promising material for optoelectronics and high-energy radiation detectors. In order to obtain a bulk single crystal from a

melt, it is crucial to understand the peculiarities of melting and crystallization processes. Here, the solid-liquid and liquid-solid phase transitions were studied by differential thermal analysis (DTA) at different heating/cooling rates (0.1, 1, 3, 5, and 10 °C/min). A two-stage melting mechanism of $CsPbBr_3$ perovskite was proposed. A critical maximal sample temperature ($T_{critical}$) was determined for each heating rate. If the sample was heated to a temperature below $T_{critical,}$ the crystallization occurred at a higher temperature than the melting point. Contrary, if the sample was heated to a temperature higher than this critical value, the melt crystallization occurred with supercooling. We believe that such crystallization features are closely related to the melt structure, which changes during the sample heating. The activation energies of melting and crystallization processes of $CsPbBr_3$ were determined as 1846 kJ/mol and 1940 kJ/mol, respectively. For the first time, this study demonstrates the impact of heating and cooling conditions on the melting and crystallization processes of the bulk $CsPbBr_3$. It is significant for fundamental crystal growth understanding and fabrication of high-quality monocrystalline material.

## INTRODUCTION

All-inorganic $CsPbBr_3$ semiconductor perovskite attracts a lot of attention nowadays. This material is very promising for use in lasers,[1-2] for manufacturing photodetectors,[3-7] X- and γ-rays detectors,[8-12] and solar cells.[13-16] Despite the wide use of low dimensional $CsPbBr_3$ in the form of nanocrystals, nanowires, and polycrystalline thin films, $CsPbBr_3$ single crystals represent the most stable form of this material. Bulk single crystals better represent the fundamental physical properties of $CsPbBr_3$ and can be more easily applied for the fabrication of photo- and ionizing radiation detectors. Crystals can be obtained by the solution growth method,[9, 17-18] but in this case, the crystal matrix may capture solvent molecules, which affects its optical and electrical properties.[9,17] The optimal way to obtain cesium lead bromide crystals is the growth from the

melt.[7,8,10,19] This method allows obtaining large in diameter single crystals with stoichiometric composition and excellent quality without organic contaminants. To grow high-quality perovskite single crystals from the melt, it is necessary to clearly understand the melting mechanism of the $CsPbBr_3$ and, even more importantly, the crystallization mechanism. Although the first work on $CsPbBr_3$ dates back to the late 19th century,[20] and the early investigations of the cesium lead bromide structure were carried out in the middle of the 20th century,[21,22] to the best of our knowledge, there are no studies on the melting and crystallization processes of the bulk $CsPbBr_3$. In several works,[23-25] authors studied low-temperature structural transformations of $CsPbBr_3$ by various methods such as neutron diffraction method, differential scanning calorimetry, thermomechanical analysis, and high-temperature X-ray diffraction, but there is minor data on solid-liquid phase transitions for $CsPbBr_3$. Cola et al.[26] investigated the CsBr – $PbBr_2$ system by differential thermal analysis (DTA) and found that the stoichiometric compound of $CsPbBr_3$ melts congruently at 567 °C. In more recent works[8,19,27] DTA method was used as a tool for melting point determination without explanations of regularities in the melting and crystallization processes of $CsPbBr_3$. The melting point was mentioned as 567 °C, but crystallization temperature varied from 514 °C[8] to 550-555 °C.[19,27] Those variations are probably due to the inconsistency in experimental conditions and different heating and cooling rates used during the measurements. In this work, we carried out the systematic study of melting and crystallization processes of all-inorganic $CsPbBr_3$ perovskite and described its phase transitions mechanism.

## EXPERIMENTAL SECTION

### Materials

Commercially available cesium bromide CsBr (99.9999%) and lead (II) bromide $PbBr_2$ (99.999%) were purchased from Sigma-Aldrich.

**$CsPbBr_3$ powder synthesis and polycrystal growth**

The synthesis of all-inorganic perovskite $CsPbBr_3$ was carried out by the mechanochemical method[8]. An equimolar quantity of CsBr and $PbBr_2$ was carefully ground and mixed in a mortar with a pestle at room temperature. Immediately after mixing began, the color of the powder gradually changed from white to saturated orange, indicating a solid-state synthesis reaction. 20 g of obtained $CsPbBr_3$ powder was loaded into a quartz ampoule, evacuated to $10^{-4}$ mbar, and sealed. Then the ampoule was placed in a furnace and heated to 640 ° C, exceeding the cesium bromide melting point. At this temperature, the melt was held for several hours and then cooled to room temperature for 20 hours.

**X-ray Diffraction (XRD) measurements**

X-ray diffraction analysis was performed by classical ex-situ Bragg – Brentano geometry using a PANalyticalX'pert powder diffractometer with filtered Cu-Kα radiation and an X'Celerator solid-state stripe detector. For measurements, polycrystalline $CsPbBr_3$ was ground into powder and placed on a zero background silicon wafer.

**Differential thermal analysis (DTA)**

500 mg of CsPbBr3 sample for the DTA experiment was loaded into a specially designed quartz ampoule (Supporting Information Figure S1a) and sealed under $10^{-4}$ mbar pressure. Measurements are performed on an in-house-built automated DTA setup with S-type thermocouples (Figure S1b). During experiments, the heating/cooling of samples was performed at different rates: 0.1, 1, 3, 5, and 10 °C/min, respectively. Measurements were carried out cyclically. The first cycle was started from room temperature, but all following cycles were performed starting from 450 °C. During recurring heatings and coolings, the maximal sample temperature increased step by step from the melting point of cesium lead bromide to ~590 °C. We fixed the melting and crystallization

temperature of $CsPbBr_3$ and temperatures of minimum and maximum on peaks on the thermograms in each cycle. The time of these points on thermograms was also recorded. Every measurement was repeated thrice.

**RESULTS AND DISCUSSION**

Obtained polycrystalline cesium lead bromide was investigated using an XRD-analysis, which confirmed the perovskite orthorhombic crystalline structure (Figure S2.).

During the DTA experiment at different conditions, we determined the melting and crystallization temperature of $CsPbBr_3$ by a baseline bend on the thermograms (Figure 1). In all cases melting point was in the range from 567 to 568.5 °C, which is in good agreement with previously published data.[8,19, 26,27] Considering in detail the process of perovskite melting, we have observed the phase transition that occurs differently on the different heating rates. In particular, it is related to the melting process duration. In the case of heating rate 0.1 °C / min, the process takes about 60 min. In the heating rate of 1 °C/min, the melting process duration was about ~ 12 min and decreased to ~ 3 min with an increase in heating rate up to 10 °C/min. The melting process duration was determined on thermograms as a difference between melting peak minimum time and baseline bend time, indicating the melting process's start. Based on these results, it can be assumed that the melting process of $CsPbBr_3$ is not isothermal, and it occurs within a specific temperature range. Depending on heating conditions, this range may change from interval of 567-574 °C for 0.1 °C/min to 567-591 °C for 10 °C/min. Slow heating rate (0.1 °C/min), which is closest to equilibrium conditions (Fig. 1 a), clearly shows that the endothermic melting peak is stretched in time, but it is less pronounced than in cases with faster heating (Fig. 1 b-e).

Particular attention should be paid to an additional slope on the melting peak on the thermograms, which is present in all cases. We can see some changes in the starting temperature

of this slope. Thus, it is fixed at 572 °C and 577 °C at the heating rates of 0.1 °C/min and 1 °C/min respectively. As the heating rate increases to 3, 5, and 10 °C/min, this temperature shifts to ~581 °C and keep constant. Change in the curvature of the line in differential thermocouple signal record during the melting process may indicate a two-step melting mechanism of $CsPbBr_3$ perovskite. It can be similar to other semiconductors such as CdTe or Cd(Zn)Te, when the solid phase fragmentation first occurs and then, with continued heating, the melting of these residues of the crystalline structure predominates.[28,29] After that, the melt becomes homogenous.

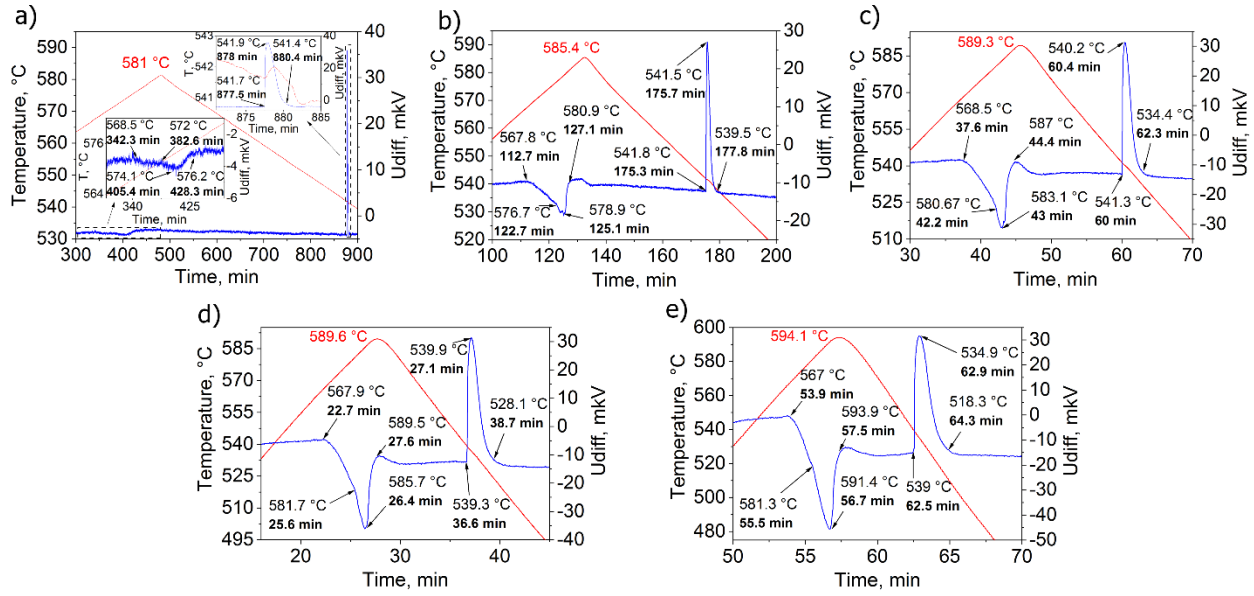


**Figure 1.** Melting and crystallization thermograms of $CsPbBr_3$ at different heating / cooling rates: a) 0.1 °C/min; b) 1 °C/min; c) 3 °C min; d) 5 °C/min; e) 10 °C/min. Red lines represent temperature changes during measurements and blue lines – the differential thermocouple voltage record.

The heating/cooling rate and melting process features have a direct impact on the sample crystallization process. Figure 1a-e represents the peculiarities of the $CsPbBr_3$ melting and crystallization processes in the conditions when the sample was heated above the melting point (567-568 °C) by ~15-20 °C, and the melting process was completed (record of the full melting peak on thermograms). Another situation is when the melting process was incomplete during the

heating (record of the incomplete melting peak on thermograms). In that case, the melt crystallizes at the same temperature from which the sample cooling was started (Figure 2).

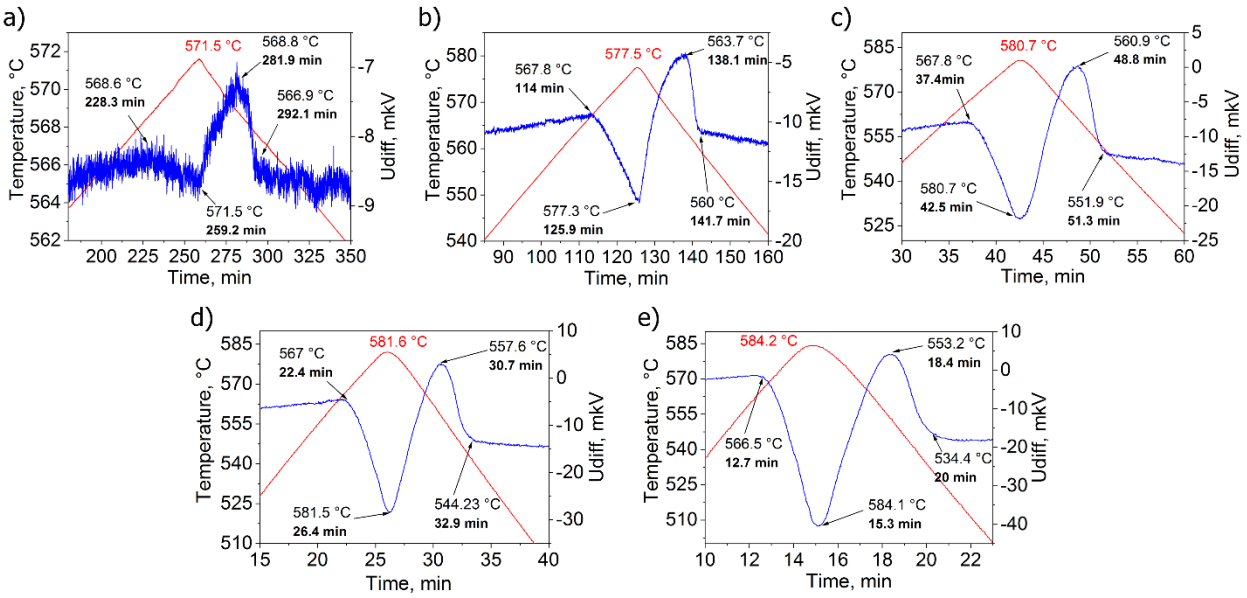


**Figure 2.** Melting and crystallization thermograms of $CsPbBr_3$ with low superheating at different heating/cooling rates: a) 0.1 °C/min; b) 1 °C/min; c) 3 °C min; d) 5 °C/min; e) 10 °C/min. Red lines represent temperature changes during measurements, blue lines – the differential thermocouple voltage record.

In that case, we observed a "hot" crystallization when the temperature of the crystallization start point is higher than the point of the melting start. It is in good agreement with the two-stage mechanism of melting proposed above. Fragments of solid-phase which are present in the melt become centers of crystallization and promote the crystallization process immediately after the start of cooling. It is typical for all investigated heating rates from 0.1 °C / min to 10 °C / min with a low superheating degree. On the other hand, if heating continues to higher temperatures, we get an opposite situation when the melt crystallizes with supercooling when sample cooling (Figure 3). The crystallization temperature of $CsPbBr_3$ is weakly dependent on the maximum sample

temperature and heating rate if superheating achives a specific defined value. This value of maximal sample temperature we called "critical temperature" ($T_{critical}$), after which the melt of the perovskite crystallizes in a narrow range temperature with practically permanent supercooling. In Figure 3, the melt crystallization in such conditions characterizes by complete exothermic peaks , which observes at around 539-545 °C. These peaks are clearly separated in time from melting peaks depending on the heating rate and the superheating degree. Here is necessary to specify superheating ($\Delta T^{+}$), which we have calculated as a difference between the maximal sample temperature ($T_{max}$) and temperature when melting of the sample starts ($T_{melt}$):

$$\Delta T^{+} = T_{max} - T_{melt} \qquad (1)$$

and supercooling ($\Delta T^{-}$), which was calculated as a difference between the melting start temperature and crystallization start temperature ($T_{cryst}$):

$$\Delta T^{-} = T_{melt} - T_{cryst} \qquad (2)$$

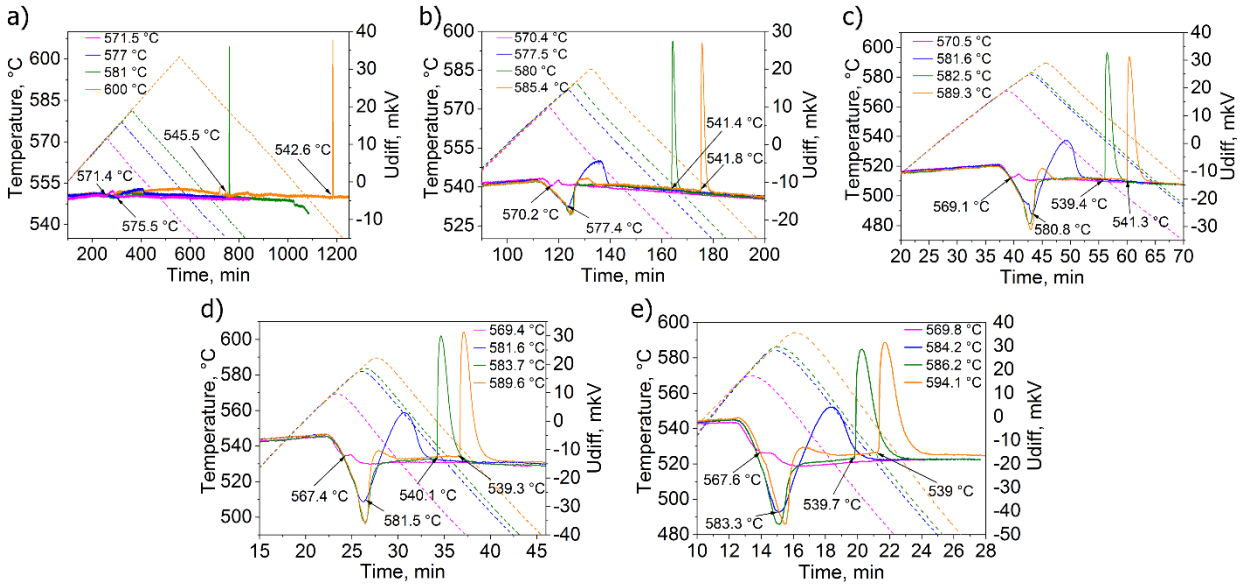


**Figure 3.** Melting/crystallization thermograms of $CsPbBr_3$ at different maximal sample temperature with heating rates: a) 0.1 °C / min., b) 1 °C / min., c) 3 °C / min., d) 5 °C/min.;

e) 10 °C/min. The peaks on the dashed lines indicate the maximal temperatures of the sample during experiments. Solid lines on all graphs are the differential thermocouple voltage records.

The temperature of $CsPbBr_3$ melt crystallization gradually increases from 568 °C to 577 °C in the case if the sample was heated to a temperature in the range from melting point temperature (~567-568 °C) to 579 °C at a heating/cooling rate of 0.1 °C/min (Figure 4a). At the same time, superheating increases, and crystallization of $CsPbBr_3$ melt occurs with supercooling in the range from 0 °C to -9 °C ("hot" crystallization). With further heating to higher temperatures, a dramatic decrease in crystallization temperature was observed. The oscillation of crystallization temperature from 543 °C to 552 °C took place when the sample was heated to a temperature greater than 579 °C. It corresponds to melt supercooling in the range from 16 °C to 25 °C. In the range of small superheating temperatures, the melting of perovskite is incomplete, and the start of the melt crystallization process is indistinct, as shown on thermograms (Figure 4a-1). It can be explained as follows: in the melt are present solid-phase fragments of different sizes, the number of which increases while approaching the critical temperature. It is caused by the splitting of large solid fragments into smaller ones. These structural units in the melt are acting as crystallization centers and trigger premature melt solidification (“hot” crystallization). After overcoming the critical superheating temperature (579 °C), $CsPbBr_3$ melts completely, and the melt becomes homogenous. Melt crystallization under these conditions is clearly shown on thermograms with supercooling (Figure 4a-2) as described above. We can also observe similar dependencies in the case of faster heating/cooling rates (Figure 4b-e). The temperature intervals of melt crystallization with supercooling are 540-550 °C for $V_{h/c}$ = 1 °C/min, 538-543 °C for $V_{h/c}$ = 3 °C/min, 537-542 °C for $V_{h/c}$ = 5 °C/min, and 538-542 °C for $V_{h/c}$ = 10 °C/min.. However, with increasing in the heating/cooling rate, a shift in $T_{critical}$ was observed. In the case of heating/cooling rate of 1 °C/min,

the same $T_{critical}$ was observed similar to 0.1 °C/min, but with $V_{h/c}$ = 3, 5 and 10 °C/min $T_{critical}$ was recorded as 582 °C, 583 °C, and 585 °C respectively (Figure 4c-e). We believe that is due to the kinetic regularities of the melting process. According to the differential thermal analysis theory,[30] melting peaks minimums on thermograms indicate full completion of the endothermic melting process. Increasing the heating rate leads to an increase of the temperatures of minimums these peaks.[30,31] The shift in critical temperature ($T_{critical}$) co-occurs with an increase of the temperature of melting peak minimum on thermograms (Figure 4f) and is apparently caused by the same kinetic patterns.

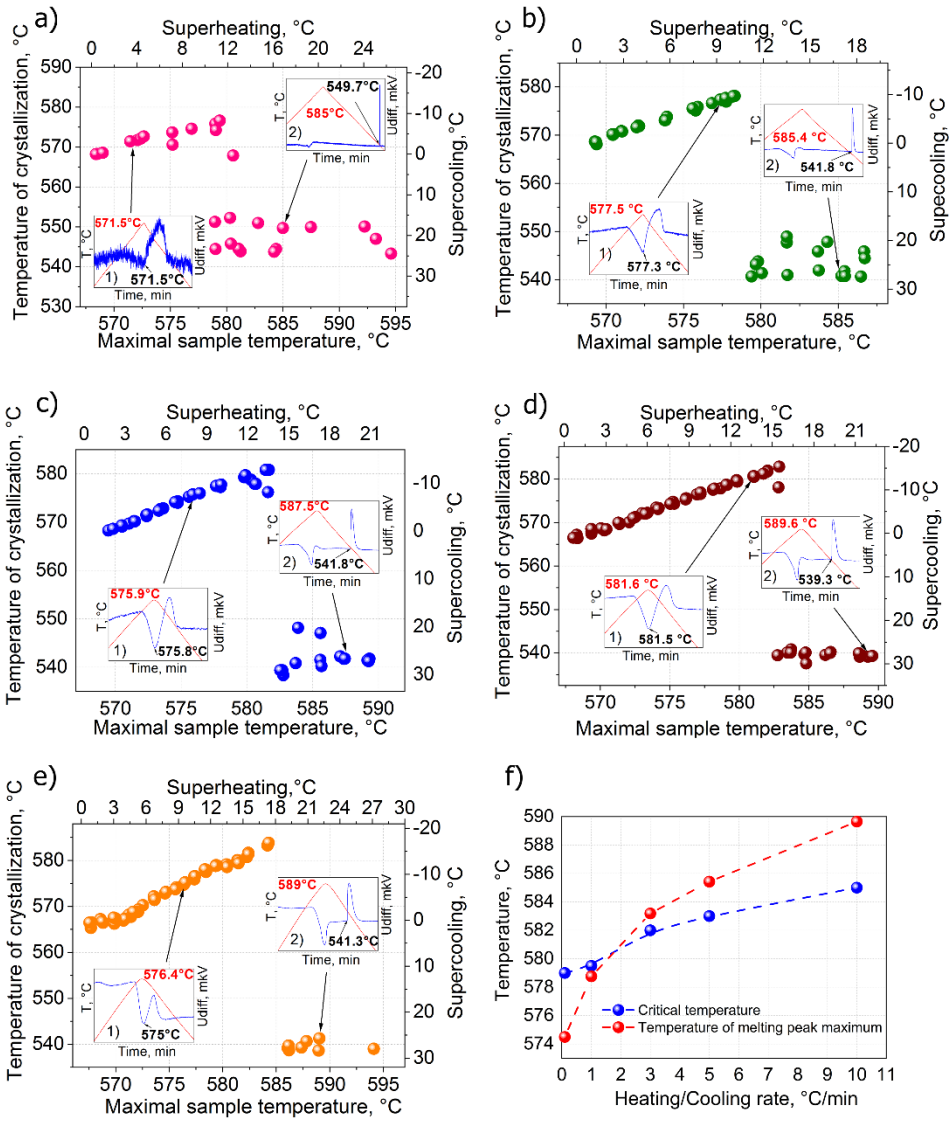

**Figure 4.** Dependences of the crystallization temperature of the $CsPbBr_3$ melt versus the maximal sample temperature and supercooling versus superheating at different heating/cooling rates: a) 0.1 °C / min., b) 1 °C / min., c) 3 °C / min., d) 5 °C/min.; e) 10 °C/min. Inserted thermograms 1) and 2) illustrate the melt crystallization with different superheating degrees (See Figure 1 and Figure 2); f) - Change in critical temperature and temperature of melting peak minimum depending on the heating rate.

Using data from thermograms after $T_{critical}$ (with complete melting and crystallization peaks) with different heating/cooling rates, the activation energy of the $CsPbBr_3$, melting $E_m$, and crystallization $E_c$ processes were estimated. Activation energy is associated with heating rates, according to the Kissinger equation:[32,33]

$$ln\frac{V_h}{T_p^2} = const + \frac{E_a}{RT_p} \qquad (3)$$

where $V_h$ is the heating/cooling rate, $T_p$ is the melting peak minimum or crystallization peak maximum temperature on thermograms, and $R$ is the universal gas constant. The slope of a straight line in coordinates $\ln(V_h/T_p^2)$ vs $1000/T_p$ (Figure 5) is equal to $E/R$. The calculated values of activation energy for melting and crystallization processes were 1846 kJ/mol and 1940 kJ/mol, respectively. As we can see, both values are comparable.

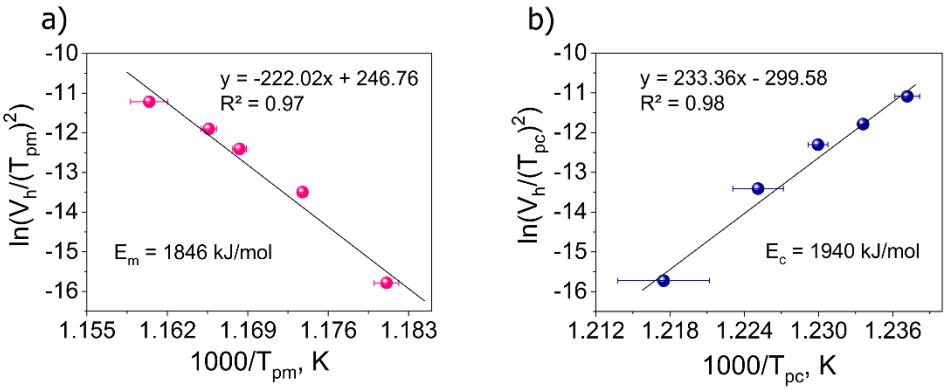

**Figure 5.** The Kissinger plots of $CsPbBr_3$ melting (a) and crystallization (b) processes. The values of the peak temperatures $T_p$ were taken from DTA thermograms with different heating/cooling rates.

Considering in more detail the crystallization process of $CsPbBr_3$ at different heating/cooling rates, we should consider the dependencies of crystallization rates ($V_{cryst}$) on temperatures to which the melt was heated before cooling down. The crystallization rate is inversely proportional to the duration of the crystallization process. It can be estimated as a reverse value of the difference between the time of crystallization peak maximum $t_{cryst}^{peak}$ and the start time of the crystallization process $t_{cryst}^{start}$:[34,35]

$$V_{cryst} = \frac{1}{t_{cryst}^{peak} - t_{cryst}^{start}} \qquad (4)$$

Figure 6 clearly shows the sharp jump of melt crystallization rate occurring at the critical temperature at all heating/cooling rates. The crystallization rate smoothly decreases in the temperature range from slight superheating (~1 °C) to critical temperatures. It was observed for all investigated cooling rates, but it is getting more pronounced with faster cooling. In small superheating, large in size residues of the crystalline phase are present in the melt and promote fast crystallization. The logical consequence is the presence of a small amount of the liquid phase in the system under these conditions. It can be evaluated by the shape and area of crystallization peak on thermograms with low sample maximal temperatures (Figure 3). When approaching the critical temperature, the crystallization rate reaches a minimal value. In these conditions, the amount of the melt increases with the simultaneous gradual fragmentation and melting of large crystalline residues. Sizes of the crystalline particles become close to critical value when they can still act as crystallization centers. At this point, the number of crystallization centers is maximal, and

crystallization occurs at the highest temperature (Figure 4). Melt is almost homogenous, and entropy at the system approaching its maximum value. Attachments of the atoms from the melt to the crystalline lattice of the existing crystal structure residues are complicated at these conditions. For this reason, the crystallization rate reaches its smallest value. Above these points, the crystalline phase remnants disappear in the melt, and there is a complete change in the crystallization mechanism. Instead of the gradual growth of crystalline remnants that goes practically without any activation barrier, the formation of new crystallization centers in the homogeneous liquid phase is required for the start of crystallization. The activation energy of this process is determined by the calculated above value. In all cases, after reaching the $T_{\text{critical}}$ the crystallization rate demonstrates values in the same range ~2-3 $\text{min}^{-1}$. These values correspond to the lowest crystallization temperatures (Figure 6b-e, Figure S3), which oscillates in the interval from 543 °C to 552 °C, as was mentioned above (Figure 4). It indicates that the cooling rate has a weak effect on the crystallization mechanism if the melt is overheated above the critical temperature. In this case, the crystallization process is determined by the homogeneous melt structure and its thermodynamic properties.

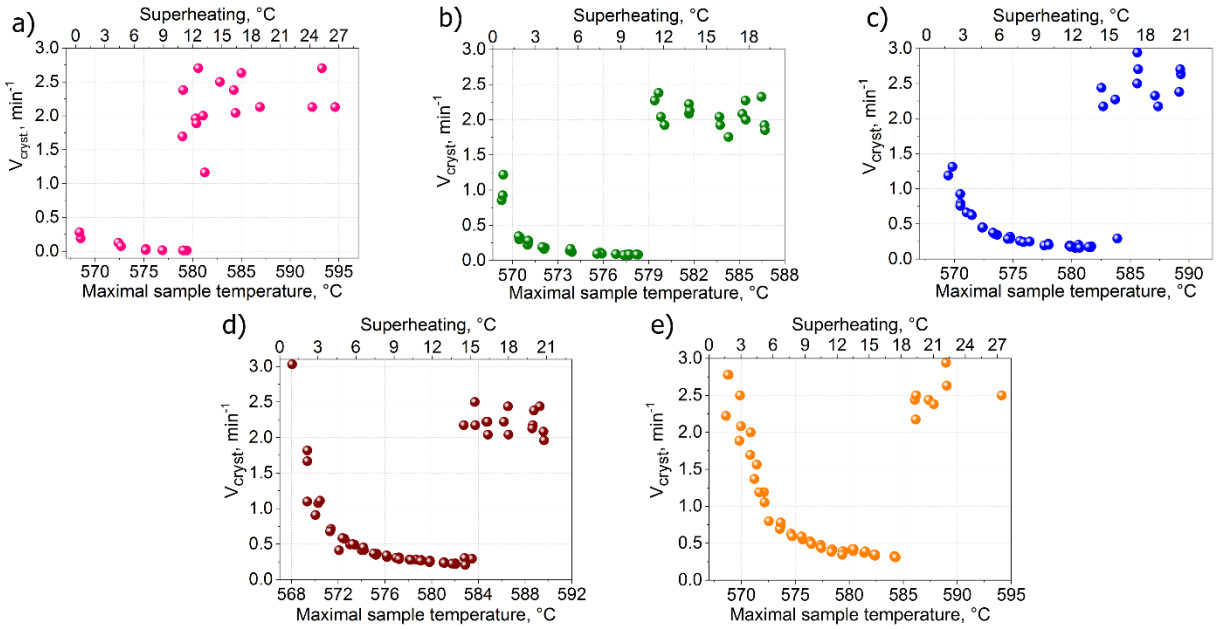


**Figure 6.** Dependencies of the $CsPbBr_3$ melt crystallization rate on the maximal sample temperature and superheating at different heating/cooling rates: a) 0.1 °C / min., b) 1 °C / min., c) 3 °C / min., d) 5 °C/min., e) 10 °C/min.

## CONCLUSION

In conclusion, we demonstrated that the melting of $CsPbBr_3$ is not an isothermal process and occurs in a defined temperature range. This range depends on heating rates and can be changed from 567-574 °C for 0.1 °C / min to 567-591 °C for 10 °C/min. The melting process of $CsPbBr_3$ occurs in two stages. The first stage is the solid phase fragmentation, and the second stage is the melting of crystalline structure residues. Using the Kissinger equation, activation energies of the melting $E_m$ and crystallization $E_c$ were estimated as 1846 kJ/mol and 1940 kJ/mol, respectively. We have determined the critical temperatures ($T_{critical}$) for different heating/cooling rates at which the second stage of the melting process ends and the melt becomes homogeneous (579 °C for 0.1 and 1 °C/min. and 582 °C, 583 °C, 585 °C for 3, 5 and 10 °C/min respectively). In the case of heating the sample below these values, "hot" crystallization of the melt was observed. Otherwise,

if heating was continued above $T_{critical}$, the melt of $CsPbBr_3$ crystalized in the defined temperature range (543-552 °C, 540-550 °C, 538-543 °C, 537-542 °C and 538-542 °C for heating/cooling rates 0.1, 1, 3, 5, and 10 °C/min respectively) with almost constant supercooling. Similar dependencies were found for the melt crystallization rates with different heating/cooling rates.This study helps to understand the melting and crystallization mechanisms of $CsPbBr_3$ more deeply. Our results explain the influence of heating and cooling conditions on the melt structure of CsPbBr3 and determine the temperature at which the melt becomes homogeneous. It has great significance for the growing technology of the high-quality bulk perovskite material.

ASSOCIATED CONTENT

**Supporting Information**

Photograph of the sealed quartz ampoule with the sample, Scheme of the automated DTA setup, X-ray diffraction pattern of the synthesized $CsPbBr_3$, Dependencies of the $CsPbBr_3$ melt crystallization rate on the maximal sample temperature and the crystallization temperature.

The Supporting Information is available free of charge (PDF).

AUTHOR INFORMATION

**Corresponding Author**

*E-mail: andriy.kanak@gmail.com, Tel: +380372584745.

**Author Contributions**

All authors have given approval to the final version of the manuscript.

**Notes**

The authors declare no competing financial interest.

ACKNOWLEDGMENT

This work has been partially financially supported by the MESU Grant for Young Scientists (State registration number 0119U100728).

REFERENCES

(1) Schlaus A. P.; Spencer M. S.; Miyata K.; Liu F.; Wang X.; Datta I.; Lipson M; Pan A.; Zhu X.-Y. How lasing happens in $CsPbBr_3$ perovskite nanowires. *Nat. Commun*. **2019,** DOI: 10.1038/s41467-018-07972-7.

(2) Wang X.; Chen H.; Zhou H.; Wang X.; Yuan S.; Yang Z.; Zhu X.; Ma R.; Pan A. Room-Temperature High Performance $CsPbBr_3$ Perovskite Tetrahedral Microlasers. *Nanoscale* **2019,** *11,* 2393-2400.

(3) 3.Li Y.; Shi Z.-F; Li S.; Lei L.-Z.; Ji H.-F.; Wu D.; Xu T.-T.; Tian Y.-T.; Li X.-J. High-performance perovskite photodetectors based on solution-processed all-inorganic $CsPbBr_3$ thin films. *J. Mater. Chem. C.* **2017,** *5,* 8355- 8360.

(4) Gui P.; Chen Z.; Li B.; Yao F.; Zheng X.; Lin Q.; Fang G. High-Performance Photodetectors Based on Single All-Inorganic $CsPbBr_3$ Perovskite Microwire. *ACS Photonics* **2018,** *5,* 2113-2119.

(5) Bao C.; Yang J.; Bai S.; Xu W.; Yan Z.; Xu Q.; Liu J.; Zhang W.; Gao F. High Performance and Stable All-Inorganic Metal Halide Perovskite-Based Photodetectors for Optical Communication Applications. *Adv. Mater.* **2018,** DOI: 10.1002/adma.201803422.

(6) Kang C. H.; Dursun I.; Liu G; Sinatra L.; Sun X.; Kong M.; Pan J.; Maity P.; Ooi E.-N.; Ng T. K.; Mohammed O. F.; Bakr O. M.; Ooi B. S. High-speed colour-converting photodetector with

all-inorganic $CsPbBr_3$ perovskite nanocrystals for ultraviolet light communication. *Light: Sci. Appl.* **2019,** DOI: 10.1038/s41377-019-0204-4.

(7) Song J.; Cui Q.; Li J.; Xu J.; Wang Y.; Xu L.; Xue J.; Dong Y.; Tian T.; Sun H.; Zeng H. Ultralarge All-Inorganic Perovskite Bulk Single Crystal for High-Performance Visible–Infrared Dual-Modal Photodetectors. *Adv. Optical Mater.* **2017,** DOI: 10.1002/adom.201700157.

(8) Stoumpos C. C.; Malliakas C. D.; Peters J. A.; Liu Z.; Sebastian M.; Im J.; Chasapis T. C.; Wibiwo A. C.; Chung D. Y.; Freeman A. J.; Wessels B. W.; Kanatzidis M. G. Crystal Growth of the Perovskite Semiconductor $CsPbBr_3$: A New Material for High-Energy Radiation Detection. *Cryst. Growth Des.* **2013,** *13,* 2722- 2727.

(9) Dirin D. N.; Cherniukh I.; Yakunin S.; Shynkarenko Y.; Kovalenko M.V. Solution-Grown $CsPbBr_3$ Perovskite Single Crystals for Photon Detection. *Chem. Mater.* **2016,** *28,* 8470-8474.

(10) He Y.; Matei L.; Jung H. J.; McCall K. M.; Chen M.; Stoumpos C. C.; Liu Z.; Peters J. A.; Chunk D. Y.; Wessels B. W.; Wasielewski M. R.; Dravid V. P.; Burger A.; Kanatzidis M. G. High spectral resolution of gamma-rays at room temperature by perovskite $CsPbBr_3$ single crystals. *Nat. Commun.* **2018,** DOI: 10.1038/s41467-018-04073-3.

(11) Pan L.; Feng Y.; Kandlakunta P.; Huang J.; Cao L. R. Performance of Perovskite $CsPbBr_3$ Single Crystal Detector for Gamma-Ray Detection. *IEEE Trans. Nucl. Sci.* **2020,** *67,* 443-449.

(12) Matt G. J.; Levchuk I.; Knüttel J.; Dallman J.; Osvet A.; Sytnyk M.; Tang X.; Elia J.; Hock R.; Heiss W.; Brabec C. J. Sensitive Direct Converting X-Ray Detectors Utilizing Crystalline $CsPbBr_3$ Perovskite Films Fabricated via Scalable Melt Processing. *Adv. Mater. Interfaces* **2020,** DOI: 10.1002/admi.201901575.

(13) Liang J.; Wang C.; Wang Y.; Xu Z.; Lu Z.; Ma Y.; Zhu H.; Hu Y.; Yi X.; Zhu G.; Lv H.; Ma L.; Chen T.; Tie Z.; Jin Z.; Liu J. All-Inorganic Perovskite Solar Cells. *J. Am. Chem. Soc.* **2016,** *138,* 15829-15832.

(14) Yuan H.; Zhao Y.; Duan J.; Wang Y.; Yang X.; Tang Q. All-inorganic $CsPbBr_3$ perovskite solar cell with 10.26% efficiency by spectra engineering. *J. Mater. Chem. A,* **2018,** *6,* 24324-24329.

(15) Li X.; Tan Y.; Lai H.; Li S.; Chen Y.; Li S.; Xu P.; Yang J. All-Inorganic $CsPbBr_3$ Perovskite Solar Cells with 10.45% Efficiency by Evaporation-Assisted Deposition and Setting Intermediate Energy Levels *ACS Appl. Mater. Interfaces* **2019,** *11,* 29746-29752.

(16) Li J.; Gao R.; Gao F.; Lei J.; Wang H.; Wu X.; Li J.; Liu H.; Hua X.; Liu S. Fabrication of efficient $CsPbBr_3$ perovskite solar cells by single-source thermal evaporation *J. Alloys Compd.* **2020,** *818,* DOI: 10.1016/j.jallcom.2019.152903.

(17) Rakita Y.; Kedem N.; Gupta S.; Sadhanala A.; Kalchenko V.; Böhm M. L.; Kulbak M.; Friend R. H.; Cahen D.; Hodes G. Low-Temperature Solution-Grown $CsPbBr_3$ Single Crystals and Their Characterization. *Cryst. Growth Des.* **2016,** *16,* 5717-5725.

(18) Saidaminov M. I.; Haque M. A., Almutlaq J.; Sarmah S.; Miao X.-H.; Begum R.; Zhumekenov A. A.; Dursun I.; Cho N.; Murali B.; Mohammed O. F.; Wu T.; Bark O. M. Inorganic Lead Halide Perovskite Single Crystals: Phase-Selective Low-Temperature Growth, Carrier Transport Properties, and Self-Powered Photodetection. *Adv. Optical Mater.* **2017,** DOI: 10.1002/adom.201600704.

(19) Zhang M.; Zheng Z.; Fu Q.; Chen Z.; He J.; Zhang S.; Chen C.; Luo W. Synthesis and single crystal growth of perovskite semiconductor $CsPbBr_3$. *J. Cryst. Growth* **2018,** *484* (Febr 15), 37-42.

(20) Wells H. L. Über die Cäsium- und Kalium-Bleihalogenide. *Z. Anorg. Chem.* **1893,** *3,* 195-210.

(21) Moller C. K. Crystal Structure and Photoconductivity of Cesium Plumbohalides. *Nature* **1958,** *182,* 1436.

(22) Sakata M.; Nishiwaki T.; Harada J. Neutron Diffraction Study the Structure of Cubic $CsPbBr_3$. *J. Phys. Soc. Jpn.* **1979,** *47,* 232-233.

(23) Hirotsu S.; Harada J.; Iizumi M.; Gesi K. Structural Phase Transitions in $CsPbBr_3$. *J. Phys. Soc. Jpn.* **1974,** *37,* 1393-1398.

(24) Hirotsu S.; Suzuki T. Critical thermodynamic properties around the successive phase transitions of $CsPbBr_3$ and $CsPbCl_3$. *Ferroelectrics* **1978,** *20,* 179-180.

(25) Rodová M.; Brozek J.; Knízek K.; Nitsh K. Phase transitions in ternary Caesium Lead Bromide. *J. Therm. Anal. Calorim.* **2003,** *71,* 667-673.

(26) Cola M.; Massarotti V.; Riccardi R.; Sinistri C. Binary Systems Formed by Lead Bromide with (Li, Na, K, Rb, Cs and Tl)Br: a DTA and Diffractometric Study. *Z. Naturforsch. A* **1971,** *26,* 1328-1332.

(27) Zhang M.; Zheng Z.; Fu Q.; Chen Z.; He J., Zhang S.; Yan L.; Hu Y.; Luo W. Growth and characterization of all-inorganic lead halide perovskite semiconductor $CsPbBr_3$ single crystals. *CrystEngComm.* **2017,** *19,* 6797-6803.

(28) Shcherbak L.; Feichouk P.; Panchouk O. Effect of CdTe "postmelting". *J. Cryst. Growth* **1996,** *161* (Apr 1), 16-19.

(29) Shcherbak L.P.; Kopach O.V.; Fochuk P.M.; Kanak A. I.; Bolotnikov A. E.; James R. B. Melting and cooling processes in CdTe-ZnTe near the CdTe-rich side. *Proc. SPIE 8142, Hard X-Ray, Gamma-Ray, and Neutron Detector Physics XIII,* San Diego, CA, September 27, 2011; SPIE: Bellingham, WA, 2011; p 81421L.

(30) Wendlandt, W W. In *Thermal analysis*, 3nd ed.; Elving P. J., Winefordner J. D., Kolthoff I. M., Eds.; Wiley-Interscience publication: New York, 1986; 19, 213-293.

(31) Melling R.; Wilburn F. W.; McIntosh R. M. Study of thermal effects observed by differential thermal analysis. Theory and its application to influence of sample parameters on a typical DTA curve. *Anal. Chem.* **1969,** *41,* 1275-1286.

(32) Kissinger H. E. Reaction kinetics in differential thermal analysis. *Anal Chem.* **1957,** *29,* 1702-1706.

(33) Zhang Z.; Chen J.; Liu H.; Xiao C. Applicability of Kissinger model in nonisothermal crystallization assessed using a computer simulation method. *J. Therm. Anal. Calorim.* **2014,** *117,* 783-787.

(34) Shcherbak L.; Feychuk P.; Kopach O.; Panchuk O.; Hayer E.; Ipser H. Fine structure of the melting process in pure CdTe and in CdTe with 2 mol% of Ge or Sn. *J. Alloys Compd.* **2003,** *349,* 145-151.

(35) Shcherbak L.; Kopach O.; Fochuk P. Solid↔liquid Cd(Zn)Te phase transition correlative analysis. *J. Cryst. Growth* **2011,** *320* (Apr 1), 6-8.

For Table of Contents Use Only

Melting and crystallization features of $CsPbBr_3$ perovskite

*Andrii Kanak*, Oleg Kopach, Liliia Kanak, Ievgen Levchuk, Mykola Isaiev, Christoph J. Brabec, Petro Fochuk, Yuriy Khalavka*

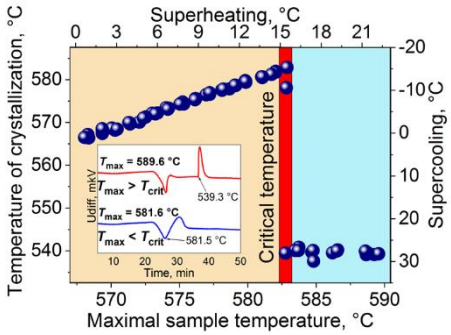


SYNOPSIS

We have investigated the melting and crystallization regularities of all-inorganic perovskite $CsPbBr_3$ by differential thermal analysis (DTA) with different heating/cooling rates (0.1, 1, 3, 5, and 10 °C/min). The impact of maximal sample heating temperature on the melt crystallization process has been shown. Here, we have proposed the two-stage mechanism of the $CsPbBr_3$ melting process and determined the "critical" heating temperature above which the melting process is completed. Using data from DTA-thermograms, we have evaluated activation energies of melting and crystallization processes of Cesium Lead Bromide as 1846 kJ/mol and 1940 kJ/mol, respectively.

Supporting Information

# Melting and crystallization features of $CsPbBr_3$ perovskite

*Andrii Kanak[1]*, Oleg Kopach[1], Liliia Kanak[1], Ievgen Levchuk[2],Mykola Isaiev[3], Christoph J. Brabec[2,4], Petro Fochuk[1], Yuriy Khalavka[1]*

*[1]Yuriy Fedkovych Chernivtsi National University, Department of General Chemistry and Chemistry of Materials, 2 Str. Kotsyubynsky, 58002, Chernivtsi, Ukraine*
*[2]Institute of Materials for Electronics and Energy Technology (i-MEET), Department of Materials Science and Engineering, Friedrich-Alexander University Erlangen-Nürnberg, Martensstrasse 7, 91058, Erlangen, Germany*
*[3]Université de Lorraine, CNRS, LEMTA, F-54000 Nancy, France*
*[4]Helmholtz-Institute Erlangen-Nürnberg for Renewable Energy (HI ERN), Immerwahrstr. 2, 91058, Erlangen, Germany*

**Corresponding Author**

*E-mail: andriy.kanak@gmail.com, Tel: +380372584745.

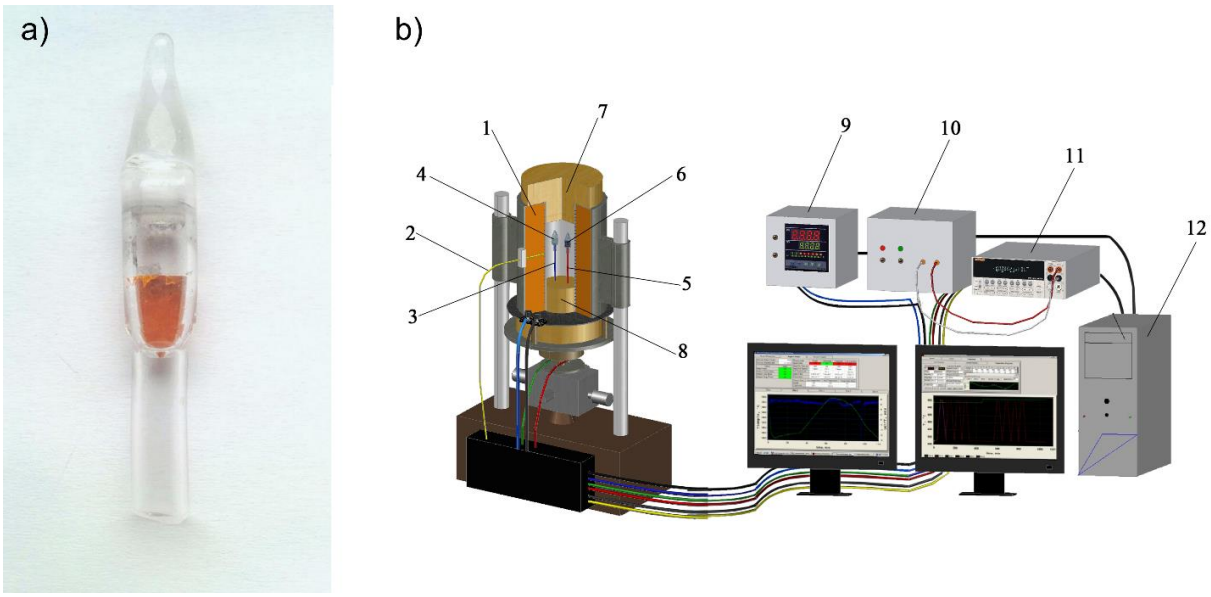


**Figure S1.** a) The sealed quartz ampoule with the sample of $CsPbBr_3$; b) The automated DTA setup:1 – the furnace; 2 – the thermocouple for furnace temperature control; 3 – the differential thermocouple; 4 – the ampoule with the reference sample; 5 – the thermocouple attached to the sample; 6 – the ampoule with the sample; 7, 8 – heat insulators; 9 – programmable thermocontroller Maxtermo MC2738; 10 – power unit and switchboard (scanner) of signals; 11 – universal digital multimeter Keithley 2000; 12 – computer.

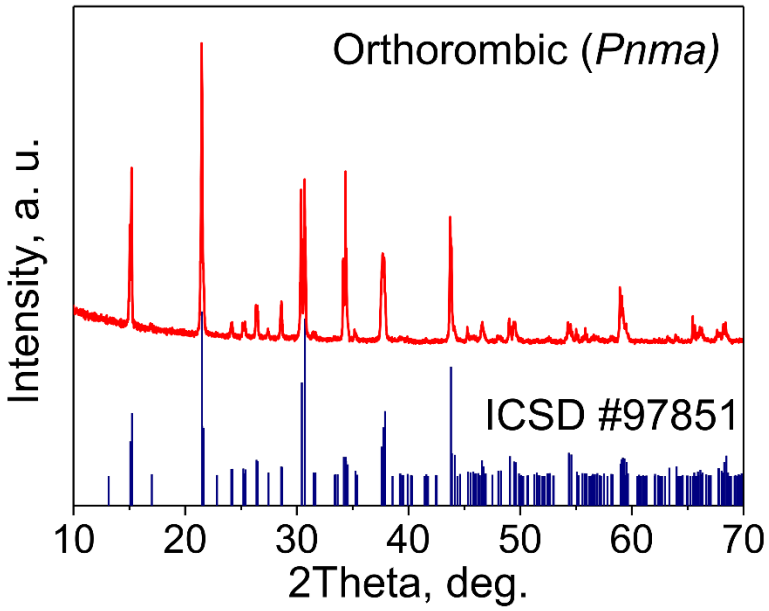


**Figure S2**. X-ray diffraction pattern of the synthesized $CsPbBr_3$. The material has an orthorhombic structure that agrees well with ICSD #97851.

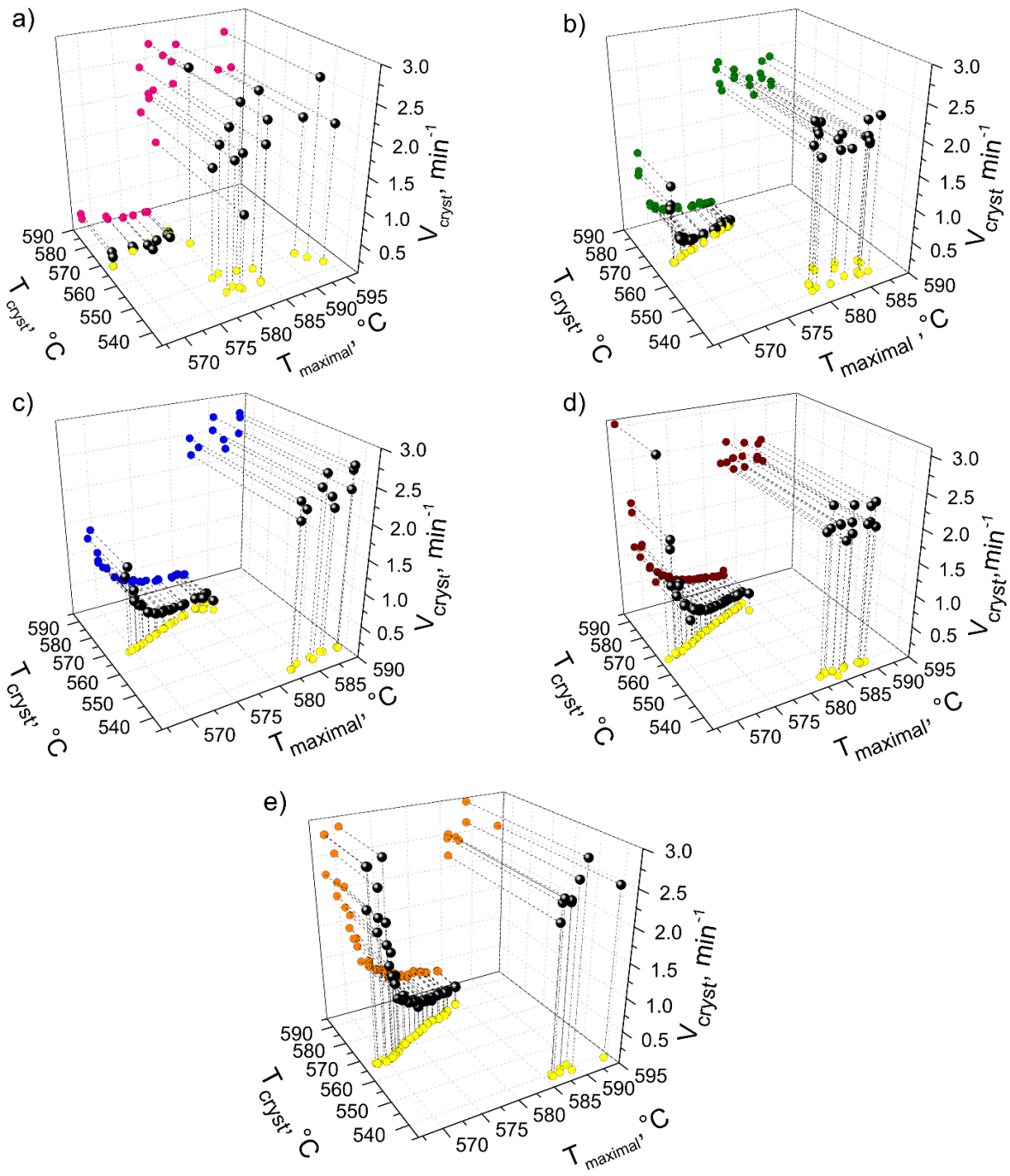


**Figure S3.** Dependencies of the crystallization rate of the $CsPbBr_3$ melt on the maximal sample temperature and the crystallization temperature at different heating/cooling rates: a) 0.1 °C / min., b) 1 °C / min, c) 3 °C / min, d) 5 °C/min, e) 10 °C/min.